Visualization of Hot Exciton Energy Relaxation from Coherent to Diffusive Regimes in Conjugated Polymers: A Theoretical Analysis

ARTICLE *in* JOURNAL OF PHYSICAL CHEMISTRY LETTERS · APRIL 2015

Impact Factor: 7.46 · DOI: 10.1021/acs.jpclett.5b00490

3 AUTHORS, INCLUDING:

Yi Zhao
Xiamen University
89 PUBLICATIONS **1,166** CITATIONS

SEE PROFILE

THE JOURNAL OF PHYSICAL CHEMISTRY Letters

Letter

pubs.acs.org/JPCL

Visualization of Hot Exciton Energy Relaxation from Coherent to Diffusive Regimes in Conjugated Polymers: A Theoretical Analysis

Yaling Ke, Yuxiu Liu, and Yi Zhao*

State Key Laboratory of Physical Chemistry of Solid Surfaces, Collaborative Innovation Center of Chemistry for Energy Materials, Fujian Provincial Key Lab of Theoretical and Computational Chemistry, and College of Chemistry and Chemical Engineering, Xiamen University, Xiamen 361005, People's Republic of China

Supporting Information

ABSTRACT: The unified coherent-to-diffusive energy relaxation of hot exciton in organic aggregates or polymers, which still remains largely unclear and is also a great challenge theoretically, is investigated from a time-dependent wavepacket diffusive approach. The results demonstrate that in the multiple time scale energy relaxation dynamics, the fast relaxation time essentially corresponds to the dephasing time of excitonic coherence motion, whereas the slow time is related to a hopping migration, and a suggested kinetic model successfully connects these two processes. The dependencies of those times on the initial energy and delocalization of exciton wavepacket as well as exciton−phonon interactions are further analyzed. The proposed method together with quantum chemistry calculations has explained an experimental observation of hot exciton energy relaxation in the low-bandgap copolymer PBDTTPD.

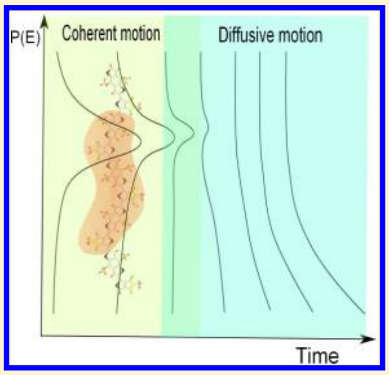

A hot exciton in organic photovoltaics usually refers to the initial excitonic state with the considerable excess energy over the mean thermal energy of vibrational motions. The energy relaxation dynamics of this hot exciton is the primary step that is crucial for controlling subsequent events such as charge separation in heterojunction solar cells and multiple exciton generation. Several experimental investigations[1−3] have suggested that the hot exciton is greatly helpful for light-to-current conversion because it can generate hot charge transfer states at the donor/acceptor interfaces, easily leading to free polaron pairs. The other studies,[4,5] however, show that the efficient charge generation is still determined by the relaxed charge transfer states at the interfaces no matter whether the exciton is hot or not. To answer the seemingly conflicting scenarios requires one to provide a direct mechanistic insight into hot exciton energy relaxation process. Because the hot exciton is a thermal nonequilibrium state, the conventional diffusive mechanism may not be suitable to explain exciton dynamics in organic crystals. Indeed, a number of recent measurements indicate that the initial energy of hot exciton immediately relaxes with a very fast rate (in femotoseconds), subsequently followed by quite slow relaxation processes.[6−13] The further investigations demonstrate that the fast evolution of exciton can greatly enhance the charge generation in donor/acceptor interfaces,[14] and the delocalized coherent motion of exciton has been proposed as a possible mechanism. The concept that the coherent motion can assist the exciton transfer has also been found in other systems, such as photosynthetic antenna complexes,[15,16] and the great effort is made to clarify coherence of exciton evolution.[17−25]

However, the hot exciton energy relaxation still remains largely unclear. In this Letter, we theoretically investigate the unified energy relaxation process of hot exciton from coherent to hoping dynamics. For the first time, we give a definite and quantitative demonstration of the intimate relationship between the ultrafast energy relaxation and dephasing of the excitonic coherence. Besides, we visualize the energy flow which is an intraband wavelike coherent motion and unveil the effect of the initial exciton properties, such as the excess energy and delocalized distribution, as well as the exciton−phonon coupling interaction on the subsequent energy relaxation dynamics, which should be very important to understand the debated observations in exciton dissociations and to reveal the ultrafast formation of interfacial charge-transfer excitons.

In typical organic polymers, the theoretical description of hot exciton evolution meets a great challenge due to the exciton−phonon interactions. The presently popular mixed quantum-classical simulations[26,27] have incorporated the exciton coherence motion; unfortunately, they usually predict an uncorrected long-time dynamics because the detailed balance principle is broken down. The alternative master equation or Monte Carlo (MC) simulation together with the nonadiabatic hopping rates[28,29] essentially neglects the coherent exciton motion. In the other direction, rigorous quantum dynamics methods still face catastrophic failure in numerical convergence when applied to nanoscale polymers. Recently, we have proposed an approximate stochastic scheme called time-

Received: March 9, 2015
Accepted: April 21, 2015

DOI: 10.1021/acs.jpclett.5b00490
J. Phys. Chem. Lett. 2015, 6, 1741−1747

dependent wavepacket diffusion method (TDWPD).[30−33] The approach essentially incorporates the quantum effects; hence, it can predict the carrier dynamics excellently consistent with those from rigorous methods for small systems, whereas its calculation cost is similar to those of mixed quantum classical methods, and the long-time dynamics is also correctly predicted. The TDWPD thus seems to be a promising way for the present purpose to make a unified description of the coherent and hopping motions in nanoscaled systems. It is noted that a Monte Carlo wave function method,[34] similar to TDWPD, has been proposed to investigate exciton propagations. In this work, the TDWPD is further expanded into an energy representation for the investigation of intraband energy relaxation.

To describe exciton dynamics in the site representation of molecular arrays, the TDWPD method requires one to solve the following differential equation for exciton wave function (the details are seen in Supporting Information)

$$i\frac{\partial|\psi(t)\rangle}{\partial t} = (H_{ex} + F(t) - i\sum_n B_n^\dagger B_n \int_0^t d\tau' \alpha(\tau') e^{-iH_{ex}\tau'} B_n^\dagger B_n e^{iH_{ex}\tau'})|\psi(t)\rangle \quad (1)$$

where H_{ex} is the exciton Hamiltonian $H_{ex} = \sum_n^N E_n B_n^\dagger B_n + \sum_{n\neq m}^N V_{nm} B_n^\dagger B_m$, E_n is the exciton energy at the nth site, V_{nm} is the exciton coupling term of mth and nth sites, $B_n^\dagger$ and B_n are the exciton creation and annihilation operators, respectively. The important exciton−phonon interaction is incorporated by the random fluctuation $F(t) = \sum_n F_n B_n^\dagger B_n$, where F_n represents the energy fluctuation on the nth site, and they can be generated from the spectral density of exciton−phonon interaction $J_n(\omega) = ((\pi)/(2))\sum_j^{N_{ph}} \omega_{nj}^3 d_{nj}^2 \delta(\omega-\omega_{nj})$, ω_{nj} is the jth phonon mode frequency at the nth site and d_{nj} is the corresponding displacement of the equilibrium position of excited state from that of the ground state. Both ω_{nj} and d_{nj} can be easily obtained from electronic structure calculations. The exciton dynamics can be obtained from the coefficients $c_n(t)$ of wave function $\psi(t) = \sum_n c_n(t)|n\rangle$.

In a model demonstration, the exciton−phonon interaction is mimicked by ohmic spectral density $J(\omega) = (1/2)\pi\xi\omega e^{-\omega/\omega_c}$ where the Kondo parameter ξ characterizes the exciton−phonon coupling strength and ω_c represents the memory effect of phonon motions.[35] The corresponding reorganization energy is given by $\lambda = \xi\omega_c$. In the simulations, the polymer chain with 200 sites is used to guarantee that wavepacket does not reach the boundaries, and a common practice in a standard spin-boson-type model is inherited in this Letter to set all the parameters in the unit of excitonic coupling ($V_{i,i\pm1} = 1$).

Due to the exciton−exciton coupling V_{mn}, the band-like excitonic states may be performed in a polymer chain or aggregate from an initial laser excitation. By controlling the laser central frequency and duration, one can generate the hot exciton with a required excess energy and delocalized distribution. We use a normalized Gaussian wavepacket

$$f(E) = \frac{1}{Z} e^{-(E-\bar{E}_0)^2/2\Delta_E} \quad (2)$$

to represent the initial wave function with respect to energy E, where $\bar{E}_0$ and Δ_E are the averaged energy and the magnitude of delocalized distribution of exciton, corresponding to the laser central frequency and pulse duration, respectively, and $Z^2=\sum_E e^{-(E-\bar{E}_0)^2/\Delta_E}$. To get the corresponding initial wave function of exciton in the site representation, we make a transformation of $f(E)$ by the matrix S from the diagonalization of exciton Hamiltonian matrix $S^\dagger H_{ex} S = E$. The schematic picture is shown in Figure 1. It is noted that several experiments have proposed that the initially formed singlet exciton in tetracene may be delocalized over 10^3−10^4 sites,[37,38] and the coherence lengths with an order of 60−100 molecules in J-aggregates formed from cyanine dyes also have been reported.[36,47] On the basis of those suggestions, we choose 100 sites in the center of chain to build band-like excitonic states in the present simulations.

Figure 2a displays the time evolution of pure exciton population (without exciton−phonon interaction) starting from a typical initial wavepacket generated by an ultrafast laser pulse. Because the pure exciton dynamics does not have a dephasing source, the exciton motion is purely coherent. This coherence is obviously indicated by an interferential pattern during the evolution and the averaged energy of exciton wavepacket, defined by $\overline{E(t)} = \sum_n c_n^*(t)c_n(t)E_n$, should keep constant, as displayed in Figure 2d. After the exciton−phonon interaction is switched on, these coherent patterns disappear (see in Figure 2b and c), and the wavepackets gradually become more localized with a larger exciton−phonon interaction. This behavior can be qualitatively explained by a faster energy loss of exciton to the phonons with a larger exciton−phonon interaction, as shown in Figure 2d, leading to a smaller exciton migration velocity.

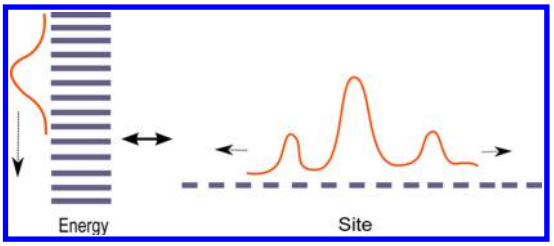

Figure 1. Transformation of initial distribution from the energy representation to the site representation. The energy band ranges from $-2V_{i,i\pm1}$ to $2V_{i,i\pm1}$ as the excitonic energies $\{E_n\}$ are all set as zero.

It is more interesting that the energy relaxation dynamics has multiple time scales. This feature has been observed by many experiments.[6,39−43] The multiexponential decay may represent different relaxation processes. Taking the decay with two characteristic times as an example, one may consider the fast decay dynamics with rate k_1 as the dephasing process whereas the slow dynamics with rate k_2 as the hopping-type motion. Qualitatively, we can kinetically explain this dynamics by a two-step process where the initial state with energy E_h goes to the intermediate state with energy E_d by dephasing, and then this state relaxes to the quasi-thermal equilibrium state with energy E_e by hopping. Under this mechanism, the energy relaxation can be expressed as follows (see in Supporting Information)

$$\bar{E}(t) = E_e + Ae^{-k_1 t} + Be^{-k_2 t} \quad (3)$$

with $A = (((E_d - E_h)\,k_1 + (E_h - E_e)k_2)C)/(k_2 - k_1)$ and $B = ((E_e - E_d)k_1 C)/(k_2 - k_1)$, where C is the initial population of exciton. Interestingly, the prefactors A and B are closely related to the state energies and rates. B is definitely positive because E_e is the equilibrium energy, which is lower than E_d, and k_1 is the faster rate constant. However, if the ratio of rate constants (k_1/

DOI: 10.1021/acs.jpclett.5b00490
J. Phys. Chem. Lett. 2015, 6, 1741−1747

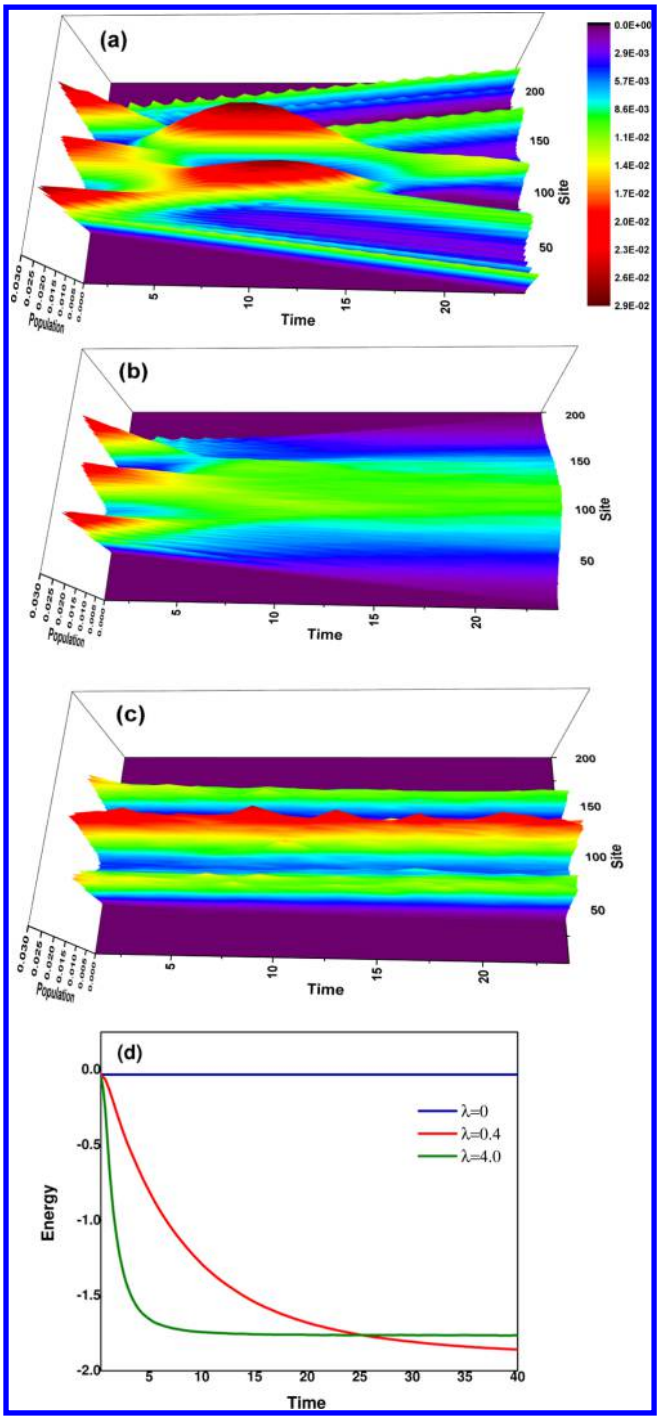

Figure 2. Exciton propagation and energy relaxation dynamics initially generated by a laser pulse with the parameters $\overline{E_0}$=0 ($2V_{i,i\pm1}$ above the bottom of energy band), Δ_E = 0.008. (a) Pure exciton dynamics without the exciton−phonon interaction. (b) and (c) Exciton propagation dynamics for the weak exciton-phonon interaction (λ = 0.4) and strong exciton−phonon interaction (λ = 4.0), respectively, where ω_c = 1 and β = 10. (d) Corresponding energy relaxations.

k_2) is larger than $((E_e - E_h)/(E_d - E_h))$, A will become negative. This behavior is also observed in the experiments.[6,39]

To investigate whether the above simple kinetic model is reasonable, one has to know the coherent property of exciton evolution to determine the dephasing time.[44,45] Here, we define coherence-length sequence $L_k(t)$

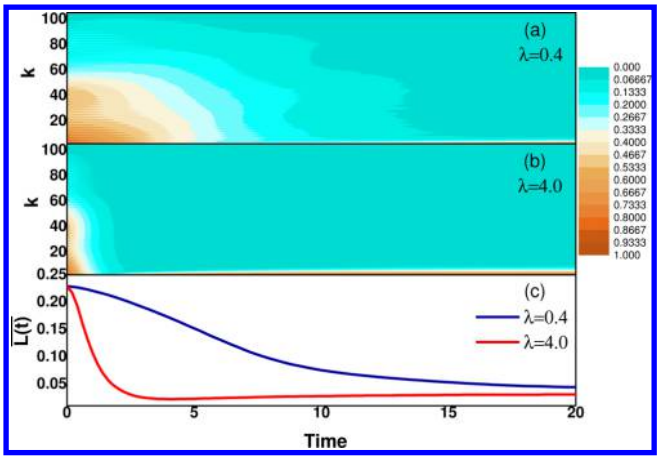

Figure 3. (a) and (b) Contour maps of coherence length sequence $\{L_k(t)\}$ with two different reorganization energies. (c) Corresponding dephasing process of the averaged coherent length $\overline{L(t)}$. The parameters are the same as those in Figure 2

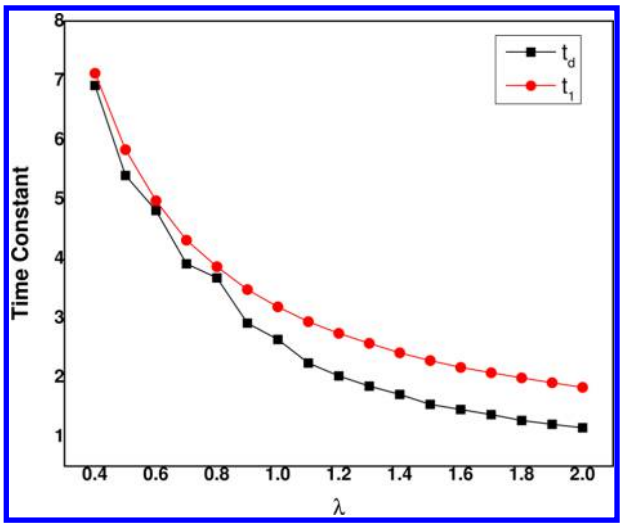

Figure 4. Dephasing time (t_d) and fast energy relaxation time (t_1) with respect to the varying reorganization energies. Other parameters are set the same as those in Figure 2.

$$L_k(t) = \sum_{i}^{N+1-k} |\langle \psi_i^*(t)\psi_{i+k-1}(t)\rangle| \quad (4)$$

where k varies from 1 to N, N is the number of site. $L_k(t)$ essentially represents the magnitude of coherence of two sites whose distance is $k - 1$. For instance, $L_1(t)$ represents the coherence of wave function of site itself and it should be 1.

Figure 3a and b display the time evolution of coherent length sequence with two different reorganization energies. Obviously, the dephasing becomes faster with a larger reorganization energy, which is in agreement with the experiments.[46] To quantitatively get the dephasing time, we calculate the averaged coherent length $\overline{L(t)} = \sum_{k=1}^{N} ((L_k)/(N - k + 1))$, and they are displayed in Figure 3c. By fitting the decay of time-dependent $\overline{L(t)}$ exponentially, we find that the dephasing time t_d is close to the fast energy relaxation time t_1 (= $1/k_1$). To further demonstrate the reliability of this relationship, we display in Figure 4 the reorganization energy dependence of these two times. It is seen that two times are consistent with each other quite well in a broad regime of exciton−phonon interactions,

DOI: 10.1021/acs.jpclett.5b00490
J. Phys. Chem. Lett. 2015, 6, 1741−1747

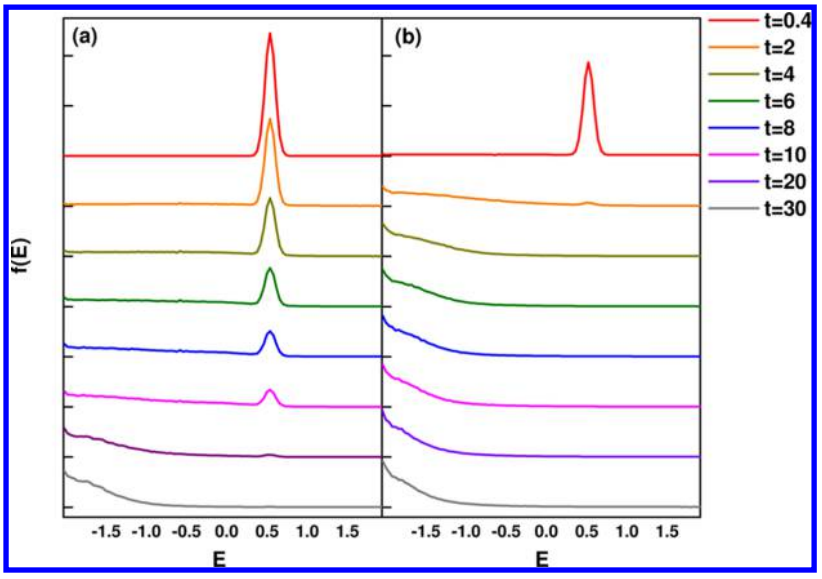

Figure 5. Exciton energy relaxation at several time snapshots in the energy representation. The left panel (a) corresponds to the reorganization energy $\lambda = 0.4$, whereas the right one (b) corresponds to $\lambda = 4$. The parameters are the same as those in Figure 2 except that $\overline{E_0}$ is set to 0.5 in order to present a more clear picture of energy relaxation dynamics.

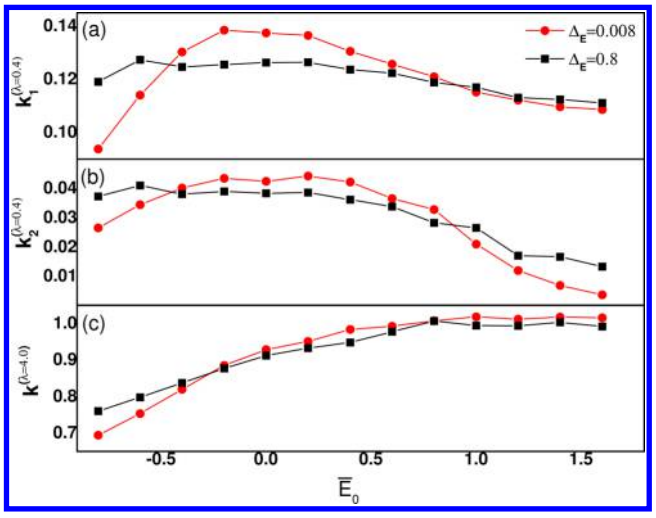

Figure 6. (a) and (b) Two energy relaxation rate constants of systems with different laser pulse duration and central frequency at the parameters $\lambda = 0.4$, $\omega_c = 1.0$, $\beta = 10$. (c) Sole energy relaxation rate constant at the parameters $\lambda = 4.0$, $\omega_c = 1.0$, $\beta = 10$.

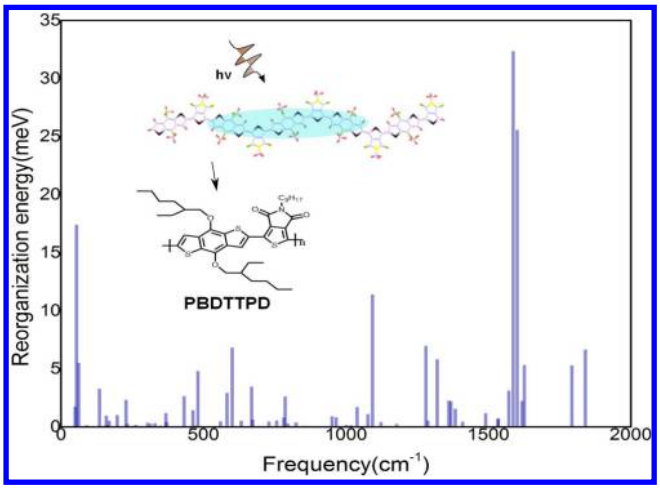

Figure 7. Frequency dependence of mode-specific reorganization energy for PBDTTPD (frequency between 3000 cm^{-1} and 3300 cm^{-1} is no showed because the peaks are too weak to display). The molecular structure and the component unit of PBDTTPD are embedded.

confirming the assumption that the fast energy relaxation corresponds to the dephasing process in the above simple kinetic model.

To see how the detailed energy components of exciton relax to the (quasi-) thermal equilibrium distribution, we transform the exciton wavepacket into the energy representation and the results at several time snapshots are displayed in Figure 5 for two different reorganization energies. Interestingly, the energy of partial wavepacket keeps a constant during the evolution, and this component may correspond to the wavelike motion observed experimentally.[12,48] The fraction of population leaked from the coherent wavepacket rapidly flow its energy into the broad of low energy levels. The successive slow hopping to the thermal equilibrium distribution then occurs among these low energy levels. For the strong exciton−phonon interaction, the time for the wavelike motion is very short, the energy relaxation is dominantly determined by the hopping process. Indeed, a single time scale can well fit the energy relaxation dynamics for $\lambda = 4$.

Now, we focus on the effect of laser frequency and pulse duration on the exciton energy relaxation dynamics. Here, we use two different pulse durations to reveal the dependence of corresponding energy relaxation dynamics on the laser frequencies. For the system with weak exciton−phonon interaction ($\lambda = 0.4$), the energy relaxations follow two exponential decays with the fast dephasing rates (k_1) ten times larger than slow diffusive rates (k_2). Figure 6 displays these two rates with respect to the initial averaged energy (laser frequency). Interestingly, there are obvious maxima for both k_1 and k_2 with use of a small value of Δ_E (= 0.008, a long pulse duration). For the dephasing process, the coherence may be maintained by the nuclear tunneling at low energies. As the energies are high enough, the exciton−phonon interaction may be considered as a perturbation and its effect on the dephasing

DOI: 10.1021/acs.jpclett.5b00490
J. Phys. Chem. Lett. 2015, 6, 1741−1747

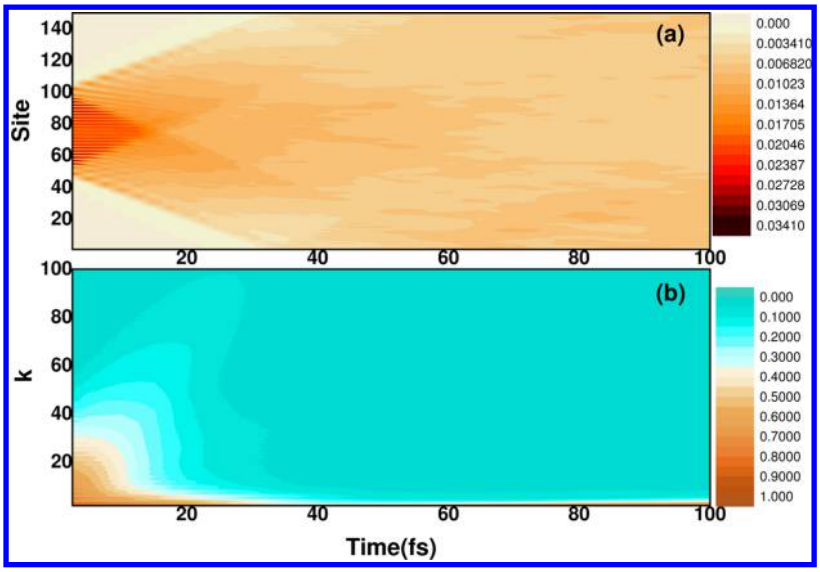

Figure 8. (a) Time-evolving exciton population of PBDTTPD at the room temperature. (b) Corresponding contour map of the coherence length sequence $\{L_k(t)\}$.

becomes smaller for the wavepacket motion with higher energies. In the intermediate energy regime, it is thus expected that the exciton−phonon interaction obviously disturbs the coherent motion of wavepacket, leading to a maximum dephasing rate k_1. The similar mechanism can explain the decreasing of k_1 in the case of $\Delta_E = 0.8$ at high energy regime, however, the coherence maintained by nuclear tunneling at low energies is not obvious because of a broad energy distribution of initial wavepacket. Because the rate k_2 corresponds to the exciton motion in a diffusive regime, it is less dependent on Δ_E, as shown in Figure 6b. The parabolic shape of rate with respect to energy may be qualitatively explained by the exciton transfer between two parabolic potentials caused by exciton−phonon interaction where the nonadiabatic transition probability has a parabolic property with respect to the energy.

In the case of strong exciton−phonon interaction, we find that a single time scale is enough to fit the energy relaxation dynamics because the dephasing time is extremely short and cannot be well fitted out. Therefore, this single rate should correspond to the diffusive motion. Indeed, the rates with different laser pulse duration are close to each other and their dependence of energy is similar to that with a weak exciton−phonon interaction, but the energy for maximum rate is shifted to a higher energy due to a higher energy barrier at the crossing point of two parabolic potentials.

The above results demonstrate that the excess energy of exciton obviously affects both the dephasing and diffusive rates, whereas the pulse duration only has a slight effect. With use of the laser with a long pulse duration, the dephasing rate of generated exciton dynamics becomes sensitive to the laser central frequency. However, how to observe this behavior experimentally is a challenge because the laser with a long pulse duration has a poor time resolution, whereas the dephasing time is very short.

In the applications to realistic aggregates or polymers, quantum chemistry calculations can be used to obtain the molecular electronic structure parameters, such as the spectral density and exciton−exciton couplings. As an example, we calculate the ultrafast exciton energy relaxation dynamics in a PBDTTPD copolymer chain that has been investigated both theoretically and experimentally as the promising conjugated polymers in organic solar cells.[49−56] The donor−acceptor fragment, shown in Figure 7, is chosen as a site. Figure 7 also shows the mode-specific reorganization energies (the detailed calculations for the spectral density and exciton−exciton coupling are described in Supporting Information). It is seen that two modes from the stretch motions of molecular skeleton with the frequencies of 1587 cm^{-1} and 1601 cm^{-1} have high contributions to the total reorganization. They may bear the major responsibility for the electron−phonon interaction and control the exciton migration rate. In the simulation of energy relaxation, the initial wave function of hot exciton is generated by an ultrafast laser pulse with 100 fs duration, and the excess energy is about 1.056 eV higher than the bottom of exciton band. After 1 ps time propagation at the room temperature (298 K), two energy relaxation times of 36 and 491 fs are obtained from energy relaxation curve. From the contours of population and coherence length sequence displayed in Figure 8, we attribute the fast time (36 fs) to the dephasing process of coherent motion, whereas the slow time corresponds to the hopping process, although the partial coherence is still maintained. Experimentally, Banerji et al.[39,49,50] have used femtosecond-resolved fluorescence up-conversion technique and global analysis to show that more than 90% of the Stoke shift takes place faster than 200 fs, the instrumental time resolution, and a characteristic time is about 500 fs, which is reported as the characteristic time for a single adjacent hopping (0.5−1 ps). From the present simulation, we suggest that the observed fast time is essentially dephasing time of exciton motion and slow one is related to hopping motion.

In summary, we have unified the coherent and hopping energy relaxation dynamics of hot exciton in organic aggregates or polymer chains. Some interesting results have been observed. For instance, the fast time scale in the energy relaxation is quantitatively assigned to the dephasing time of exciton coherent motion and a wavelike motion of exciton can only be observed in this time duration, whereas the slow energy relaxation corresponds to the hopping motion. A suggested simple kinetic model can connect the coherent and diffusive process of exciton energy relaxation. The initial energy and

DOI: 10.1021/acs.jpclett.5b00490
J. Phys. Chem. Lett. 2015, 6, 1741−1747

delocalization of exciton wavepacket, corresponding to the laser frequency and pulse duration, indeed have the effect on the energy relaxation and they can be used to optimize, especially, the dephasing time. However, the exciton−phonon interaction plays a key role in the determination of relaxation rates. The present approach may be applied to explain a broad overview of energy relaxation processes in organic aggregates, copolymers, and photosynthetic complexes.

■ ASSOCIATED CONTENT

Supporting Information

The derivation of time-dependent wavepacket method based on the Frenkel-exciton model that coupled to the harmonic baths and the kinetic model of energy relaxation process are supplied. The details of electronic structure calculations for the reorganization energy, exciton coupling, spectral density of PBDTTPD are also available. The Supporting Information is available free of charge on the ACS Publications website at DOI: 10.1021/acs.jpclett.5b00490.

■ AUTHOR INFORMATION

Corresponding Author

*E-mail: yizhao@xmu.edu.cn.

Notes

The authors declare no competing financial interest.

■ ACKNOWLEDGMENTS

The authors thank the financial supports from the National Science Foundation of China (Grant Nos. 91333101 and 21133007) and the 973 Program (2013CB834602).

■ REFERENCES

(1) Grancini, G.; Maiuri, M.; Fazzi, D.; Petrozza, A.; Egelhaaf, H. J.; Brida, D.; Cerullo, G.; Lanzani, G. Hot Exciton Dissociation in Polymer Solar Cells. *Nat. Mater.* **2013**, *12*, 29−33.

(2) Jailaubekov, A. E.; Willard, A. P.; Tritsch, J. R.; Chan, W. L.; Sai, N.; Gearba, R.; Kaake, L. G.; Williams, K. J.; Leung, K.; Rossky, P. J.; et al. Hot Charge-Transfer Excitons Set the Time Limit for Charge Separation at Donor/Acceptor Interfaces in Organic Photovoltaics. *Nat. Mater.* **2013**, *12*, 66−73.

(3) Huo, M. M.; Hu, R.; Xing, Y. D.; Liu, Y. C.; Ai, X. C.; Zhang, J. P.; Hou, J. H. Impacts of Side Chain and Excess Energy on the Charge Photogeneration Dynamics of Low-Bandgap Copolymer-Fullerene Blends. *J. Chem. Phys.* **2014**, *140*, 084903.

(4) Vandewal, K.; Albrecht, S.; Hoke, E. T.; Graham, K. R.; Widmer, J.; Douglas, J. D.; Schubert, M.; Mateker, W. R.; Bloking, J. T.; Burkhard, G. F.; et al. Efficient Charge Generation by Relaxed Charge-Transfer States at Organic Interfaces. *Nat. Mater.* **2014**, *13*, 63−68.

(5) Lee, J.; Vandewal, K.; Yost, S. R.; Bahlke, M. E.; Goris, L.; Baldo, M. A.; Manca, J. V.; Voorhis, T. V. Charge Transfer State versus Hot Exciton Dissociation in Polymer-Fullerene Blended Solar Cells. *J. Am. Chem. Soc.* **2010**, *132*, 11878−11880.

(6) Banerji, N.; Cowan, S.; Vauthey, E.; Heeger, A. J. Ultrafast Relaxation of the Poly(3-hexylthiophene) Emission Spectrum. *J. Phys. Chem. C* **2011**, *115*, 9726−9739.

(7) Scheblykin, I. G.; Yartsev, A.; Pullerits, T.; Gulbinas, V.; Sundström, V. Excited State and Charge Photogeneration Dynamics in Conjugated Polymers. *J. Phys. Chem. B* **2007**, *111*, 6303−6321.

(8) Kee, T. W. Femtosecond Pump-Push-Probe and Pump-Dump-Probe Spectroscopy of Conjugated Polymers: New Insight and Opportunities. *J. Phys. Chem. Lett.* **2014**, *5*, 3231−3240.

(9) Yang, X. J.; Dykstra, T. E.; Scholes, G. D. Photon-Echo Studies of Collective Absorption and Dynamic Localization of Excitation in Conjugated Polymers and Oligomers. *Phys. Rev. B* **2005**, *71*, 045203.

(10) Dai, D. C.; Monkman, A. P. Femtosecond Hot-Exciton Emission in a Ladder-Type π-Conjugated Rigid-Polymer Nanowire. *Phys. Rev. B* **2013**, *87*, 045308.

(11) Wells, N. P.; Blank, D. A. Correlated Exciton Relaxation in Poly(3-hexylthiophene). *Phys. Rev. Lett.* **2008**, *100*, 086403.

(12) Engel, G. S.; Calhoun, T. R.; Read, E. L.; Ahn, T. K.; Mančal, T.; Cheng, Y. C.; Blankenship, R. E.; Fleming, G. R. Evidence for Wavelike Energy Transfer through Quantum Coherence in Photosynthetic Systems. *Nature* **2007**, *446*, 782−786.

(13) Kempe, J. Quantum Random Walks: An Introductory Overview. *Contemp. Phys.* **2003**, *44*, 307−327.

(14) Kaake, L. G.; Moses, D.; Heeger, A. J. Coherence and Uncertainty in Nanostructured Organic Photovoltaics. *J. Phys. Chem. Lett.* **2013**, *4*, 2264−2268.

(15) Chenu, A.; Scholes, G. D. Coherence in Energy Transfer and Photosynthesis. *Annu. Rev. Phys. Chem.* **2015**, *66*, 69−96.

(16) Fassioli, F.; Dinshaw, R.; Arpin, P. C.; Scholes, G. D. Photosynthetic Light Harvesting: Excitons and Coherence. *J. R. Soc. Interface* **2014**, *11*, 20130901.

(17) Meier, T.; Chernyak, V.; Mukamel, S. Multiple Exciton Coherence Sizes in Photosynthetic Antenna Complexes Viewed by Pump-Probe Spectroscopy. *J. Phys. Chem. B* **1997**, *101*, 7332−7342.

(18) Dahlbom, M.; Pullerits, T.; Mukamel, S.; Sundström, V. Exciton Delocalization in the B850 Light-Harvesting Complex: Comparison of Different Measures. *J. Phys. Chem. B* **2001**, *105*, 5515−5524.

(19) Ishizaki, A.; Fleming, G. R. Theoretical Examination of Quantum Coherence in a Photosynthetic System at Physiological Temperature. *Proc. Natl. Acad. Sci. U.S.A.* **2009**, *106*, 17255−17260.

(20) Calhoun, T. R.; Fleming, G. R. Quantum Coherence in Photosynthetic Complexes. *Phys. Status Solidi B* **2011**, *248*, 833−838.

(21) Ishizaki, A.; Fleming, G. R. Quantum Coherence in Photosynthetic Light Harvesting. *Annu. Rev. Condens. Matter Phys.* **2012**, *3*, 333−361.

(22) Ishizaki, A.; Fleming, G. R. On the Interpretation of Quantum Coherent Beats Observed in Two-Dimensional Electronic Spectra of Photosynthetic Light Harvesting Complexes. *J. Phys. Chem. B* **2011**, *115*, 6227−6233.

(23) Cheng, Y. C.; Fleming, G. R. Coherence Quantum Beats in Two-Dimensional Electronic Spectroscopy. *J. Phys. Chem. A* **2008**, *112*, 4254−4260.

(24) Lee, H.; Cheng, Y. C.; Fleming, G. R. Coherence Dynamics in Photosynthesis: Protein Protection of Excitonic Coherence. *Science* **2007**, *316*, 1462−1465.

(25) Kreisbeck, C.; Kramer, T. Long-Lived Electronic Coherence in Dissipative Exciton Dynamics of Light-Harvesting Complexes. *J. Phys. Chem. Lett.* **2012**, *3*, 2828−2833.

(26) Troisi, A. Charge Transport in High Mobility Molecular Semiconductors: Classical Models and New Theories. *Chem. Soc. Rev.* **2011**, *40*, 2347−2358.

(27) Akimov, A. V.; Neukirch, A. J.; Prezhdo, O. V. Theoretical Insights into Photoinduced Charge Transfer and Catalysis at Oxide Interfaces. *Chem. Rev.* **2013**, *113*, 4496−4565.

(28) Wang, L. J.; Nan, G. J.; Yang, X. D.; Peng, Q.; Li, Q. K.; Shuai, Z. G. Computational Methods for Design of Organic Materials with High Charge Mobility. *Chem. Soc. Rev.* **2010**, *39*, 423−434.

(29) Westenhoff, S.; Daniel, C.; Friend, R. H.; Silva, C.; Sundström, V.; Yartsev, A. Exciton Migration in a Polythiophene: Probing the Spatial and Energy Domain by Line-Dipole Förster-Type Energy Transfer. *J. Chem. Phys.* **2005**, *122*, 094903.

(30) Zhong, X. X.; Zhao, Y. Charge Carrier Dynamics in Phonon-Induced Fluctuation Systems from Time-Dependent Wavepacket Diffusion Approach. *J. Chem. Phys.* **2011**, *135*, 134110.

(31) Zhong, X. X.; Zhao, Y. Non-Markovian Stochastic Schrödinger Equation at Finite Temperatures for Charge Carrier Dynamics in Organic Crystals. *J. Chem. Phys.* **2013**, *138*, 014111.

(32) Zhong, X. X.; Zhao, Y.; Cao, J. S. Coherent Quantum Transport in Disordered Systems: II. Temperature Dependence of Carrier Diffusion Coefficients from the Time-Dependent Wavepacket Diffusion Method. *New J. Phys.* **2014**, *16*, 045009.

DOI: 10.1021/acs.jpclett.5b00490
J. Phys. Chem. Lett. 2015, 6, 1741−1747

(33) Han, L.; Zhong, X. X.; Liang, W. Z.; Zhao, Y. Energy Relaxation and Separation of a Hot Electron−Hole Pair in Organic Aggregates from a Time-Dependent Wavepacket Diffusion Method. *J. Chem. Phys.* **2014**, *140*, 214107.
(34) Valleau, S.; Saikin, S. K.; Yung, M. H.; Guzik, A. A. Exciton Transport in Thin-Film Cyanine Dye J-Aggregates. *J. Chem. Phys.* **2012**, *137*, 034109.
(35) Forsythe, K. M.; Makri, N. Dissipative Tunneling in a Bath of Two-Level Systems. *Phys. Rev. B* **1999**, *60*, 972−978.
(36) Würthner, F.; Kaiser, T. E.; Saha-Möller, C. R. J-Aggregates: From Serendipitous Discovery to Supramolecular Engineering of Functional Dye Materials. *Angew. Chem., Int. Ed.* **2011**, *50*, 3376−3410.
(37) Chan, W. L.; Ligges, M.; Zhu, X. Y. The Energy Barrier in Singlet Fission can be Overcome through Coherent Coupling and Entropic Gain. *Nat. Chem.* **2012**, *4*, 840−845.
(38) Dubin, F.; Melet, R.; Barisien, T.; Grousson, R.; Legrand, L.; Schott, M.; Voliotis, V. Macroscopic Coherence of a Single Exciton State in an Organic Quantum Wire. *Nat. Phys.* **2006**, *2*, 32−35.
(39) Banerji, N.; Cowan, S.; Leclerc, M.; Vauthey, E.; Heeger, A. J. Exciton Formation, Relaxation, and Decay in PCDTBT. *J. Am. Chem. Soc.* **2010**, *132*, 17459−17470.
(40) Dykstra, T. E.; Hennebicq, E.; Beljonne, D.; Gierschner, J.; Claudio, G.; Bittner, E. R.; Knoester, J.; Scholes, G. D. Conformational Disorder and Ultrafast Exciton Relaxation in PPV-Family Conjugated Polymers. *J. Phys. Chem. B* **2009**, *113*, 656−667.
(41) Freiberg, A.; Lin, S.; Timpmann, K.; Blankenship, R. E. Exciton Dynamics in FMO Bacteriochlorophyll Protein at Low Temperatures. *J. Phys. Chem. B* **1997**, *101*, 7211−7220.
(42) Chen, K.; Barker, A. J.; Reish, M. E.; Gordon, K. C.; Hodgkiss, J. M. Broadband Ultrafast Photoluminescence Spectroscopy Resolves Charge Photogeneration via Delocalized Hot Excitons in Polymer: Fullerene Photovoltaic Blends. *J. Am. Chem. Soc.* **2013**, *135*, 18502−18512.
(43) Wells, N. P.; Boudouris, B. W.; Hillmyer, M. A.; Blank, D. A. Intramolecular Exciton Relaxation and Migration Dynamics in Poly(3-hexylthiophene). *J. Phys. Chem. C* **2007**, *111*, 15404−15414.
(44) Tempelaar, R.; Spano, F. C.; Knoester, J.; Jansen, T. L. Mapping the Evolution of Spatial Exciton Coherence through Time-Resolved Fluorescence. *J. Phys. Chem. Lett.* **2014**, *5*, 1505−1510.
(45) Spano, F. C.; Yamagata, H. Vibronic Coupling in J-Aggregates and Beyond: A Direct Means of Determining the Exciton Coherence Length from the Photoluminescence Spectrum. *J. Phys. Chem. B* **2010**, *115*, 5133−5143.
(46) Wang, T.; Chan, W. L. Dynamical Localization Limiting the Coherent Transport Range of Excitons in Organic Crystals. *J. Phys. Chem. Lett.* **2014**, *5*, 1812−1818.
(47) Whaley, K. B.; Kocherzhenko, A. A.; Nitzan, A. Coherent and Diffusive Time Scales for Exciton Dissociation in Bulk Heterojunction Photovoltaic Cells. *J. Phys. Chem. C* **2014**, *118*, 27235−27244.
(48) Dawlaty, J. M.; Ishizaki, A.; De, A. K.; Fleming, G. R. Microscopic Quantum Coherence in a Photosynthetic-Light-Harvesting Antenna. *Philos. Trans. R. Soc. A* **2012**, *370*, 3672−3691.
(49) Paraecattil, A. A.; Beaupré, S.; Leclerc, M.; Moser, J.-E.; Banerji, N. Intensity Dependent Femtosecond Dynamics in a PBDTTPD-Based Solar Cell Material. *J. Phys. Chem. Lett.* **2012**, *3*, 2952−2958.
(50) Paraecattil, A. A.; Banerji, N. Charge Separation Pathways in a Highly Efficient Polymer: Fullerene Solar Cell Material. *J. Am. Chem. Soc.* **2014**, *136*, 1472−1482.
(51) Guo, Z.; Lee, D.; Schaller, R. D.; Zuo, X.; Lee, B.; Luo, T.; Gao, H.; Huang, L. Relationship between Interchain Interaction, Exciton Delocalization, and Charge Separation in Low-Bandgap Copolymer Blends. *J. Am. Chem. Soc.* **2014**, *136*, 10024−10032.
(52) Hwang, I.; Beaupré, S.; Leclerc, M.; Scholes, G. D. Ultrafast Relaxation of Charge-Transfer Excitons in Low-Bandgap Conjugated Copolymers. *Chem. Sci.* **2012**, *3*, 2270−2277.
(53) Risko, C.; McGehee, M. D.; Brédas, J.-L. A Quantum-Chemical Perspective into Low Optical-Gap Polymers for Highly-Efficient Organic Solar Cells. *Chem. Sci.* **2011**, *2*, 1200−1218.
(54) Zhang, Y.; Hau, S. K.; Yip, H.-L.; Sun, Y.; Acton, O.; Jen, A. K.-Y. Efficient Polymer Solar Cells Based on the Copolymers of Benzodithiophene and Thienopyrroledione. *Chem. Mater.* **2010**, *22*, 2696−2698.
(55) Zou, Y.; Najari, A.; Berrouard, P.; Beaupré, S.; Réda Aïch, B.; Tao, Y.; Leclerc, M. A Thieno[3, 4-*c*]pyrrole-4,6-dione-Based Copolymer for Efficient Solar Cells. *J. Am. Chem. Soc.* **2010**, *132*, 5330−5331.
(56) Van den Brande, N.; Van Lier, G.; Da Pieve, F.; Van Assche, G.; Van Mele, B.; De Proft, F.; Geerlings, P. A Time Dependent DFT Study of the Efficiency of Polymers for Organic Photovoltaics at the Interface with PCBM. *R. Soc. Chem. Adv.* **2014**, *4*, 52658−52667.

DOI: 10.1021/acs.jpclett.5b00490
J. Phys. Chem. Lett. 2015, 6, 1741−1747